Discussion of analysis procedure
(updated after meeting)

David Bowman

6/20/16 3He analysis meeting

Goals of the Analysis Procedure

Analyze n^3He data to produce valid asymmetries and uncertainties with cuts that are motivated by the properties of the apparatus, beam, and n^3He physics and that have minimal operator discretion.

Chopper phase cut

NPDgamma, we calculated the chopper phases by looking at the initial rise and final fall of the neutron yield vs. time bin. We solved for the time at which the yield vs. time crossed half the maximum yield. For NPDgamma a small fraction of the data were rejected by the chopper phase cut. Because of the difficulty of determining the polarization for runs with the choppers unlocked, the only recourse is to cut such runs.

If a neutron passes through the spin flipper when the spin flipper is off, the neutron polarization is unchanged. When the spin flipper is on, neutrons are rotated by calculable amounts. Starting from a perfect pulse and knowledge of the spin flipper RF field strength as a function of time, one can determine the polarization for prompt as well as wrap-around neutrons. Approximately 10% of the neutrons have wrapped around. The corrections to the polarization are ~ few %.

Statistical properties of A and B type run sequences

We are now analyzing type A and type B runs separately. We need to determine if the probability of getting a type A run is independent of the history of run types. The simplest situation would be that the type of each run was independent of the type history and that A and B runs were equally probable. We could investigate this question by finding a long uninterrupted sequence of runs and assigning a 1 or -1 to types A and B. If the auto correlation of the sequence is a delta function, then we have independence of history. If not, we need to find out what governs the probability of A and B.

Physics (P) and Machine (M) asymmetries

We are now taking 600 pulse sequences as the objects to be analyzed for asymmetries, PV or PA. Every run consists of =42 600-t0 sequences. In a given run, the first pulse after every deliberately dropped pulse is always spin up (type A) or always spin down (type B). There are two types of asymmetries in the data;
1. Asymmetries caused by the interaction of the neutron with the ^{3}He target (P=physics asymmetries).
2. Asymmetries caused by the change in beam properties caused by deliberately dropping pulses, (M=machine asymmetries). In the above analysis, the only feature that showed an M type asymmetry was a dependence of the monitor yield as a function of pulse number after the dropped pulse. The intensity changed by approximately 10^{-3} in 10 seconds, the duration of a spin sequence. The intensity variation causes an average false asymmetry of $\sim 0.6\ 10^{-6}$ for a sequence. Neither the P or M asymmetries showed the "horn" feature. An important difference in the present analysis and analyses performed earlier is that in the present analysis the DC offsets for each detector were subtracted before forming the asymmetries. It may be that the DC offsets caused the horns.

The average asymmetry of type A runs is M+P and the average for type B runs is M-P. If both P and M enter the value of the measured linearly, then M=(A+B)/2 and P=(A-B)/2. Kabir analyzed approximately 30,000 runs that had no randomly dropped pulses and determine the M and the PV n^{3}He asymmetry and 1000 runs to determine the M and PA n^{3}He asymmetry. The results were:

PV = $(1.1 \pm .9)\ 10^{-8}$
PC = $(-43 \pm 5)\ 10^{-8}$

Dropped Pulse Cuts

A substantial fraction of sequences have dropped pulses. I argue that we should establish a criterion for identifying and cutting dropped pulses. For example, for each run we determine the maximum intensity of all pulses and then histogram the ratio of each pulse to that of the maximum pulse (fractional intensity). From the fractional intensity histogram, we could determine the fractional intensity for which the number of events is minimal and take this fractional to be the cut level.

The definition of the physics asymmetry is P=(A-B)/2. Dropped pulses in A and B runs will affect P oppositely. The average value of P is not shifted by cutting dropped pulse pairs. However, cutting dropped pulse pairs will affect the fluctuations in P from sequence to sequence and run to run. dropped pulses in B runs.

Recall that the change in the asymmetry of a pulse pair is ~ 0.6 10^{-6}. I estimated the statistical uncertainty in a pulse pair from the statistical uncertainty in the PV asymmetry:

$$\sigma_{PV} = \sigma_{Pair} \frac{1}{\bar{G}} \sqrt{\#\, \det ectors \times \# Runs \times \# Pulse\ Pairs / Run}$$

$$\sigma_{Pair} = 10^{-4}$$

The change in P for a randomly dropped pulse pair is 2 orders of magnitude smaller than the statistical fluctuations in a pair asymmetry. Therefore the uncertainty determined from sequences with randomly dropped pulses is expected to be the approximately same as for perfect sequences.

Conclusion

The analysis procedures discussed above will produce valid physics asymmetries and uncertainties. There are few if any personal choices to be made in the analysis.

Loose Ends

1. Include correlations between detector signals in the analysis. Develop theory of correlations.
2. Calculate average polarization including wrap-around neutrons.
3. Develop intensity cut algorithm for dropped pulses. Histogram the relative intensities for many runs. Find relative intensity for which the yield is minimum. Can we find a universal intensity cut criterion?

4. Demonstrate that “horn” feature was indeed caused by not subtracting DC offsets from detector signals.
5. Perform separate analyses of data for A. runs with and without randomly dropped pulses, B. for the first 20 pulse pairs and the last 279 pulse pairs. Compare results of the 2 pairs of results.
6. Analyze jaw-scan data. Does the range-energy relationship we are using predict the observed jaw-scan data? Does the jaw-scan data depend on beam intensity?
7. Compare detector asymmetry results for high and low-intensity runs. Carry out analyses with different range-energy curves.

Further discussion of 6.

6A.
The object of 6. Is to test our ability to calculate the geometric factors, g’s. The g’s depend on the trajectories, ranges, dedx… od protons and tritons in He. The yields from the jaw scan runs depend on the same factors.

John Calarco has convincingly argued that the dE/dX of protons in He depends only on the ratio of the E/m (velocity) in the laboratory frame.

The figure shows a proton track that begins at the end with no arrow and ends at the arrow tip. To calculate geometric factors and yields, we need to calculate the energy deposited in each cell. The deposited energy does depend on the mass of the hydrogen isotope, 1 or 3 for the n-^{3}He experiment. The simplest way of calculating the deposited energy is to determine the residual ranges, R1 and R2, at which the hydrogen ion enters and leaves a cell. Then,

$$\Delta E = E(R1) - E(R2)$$

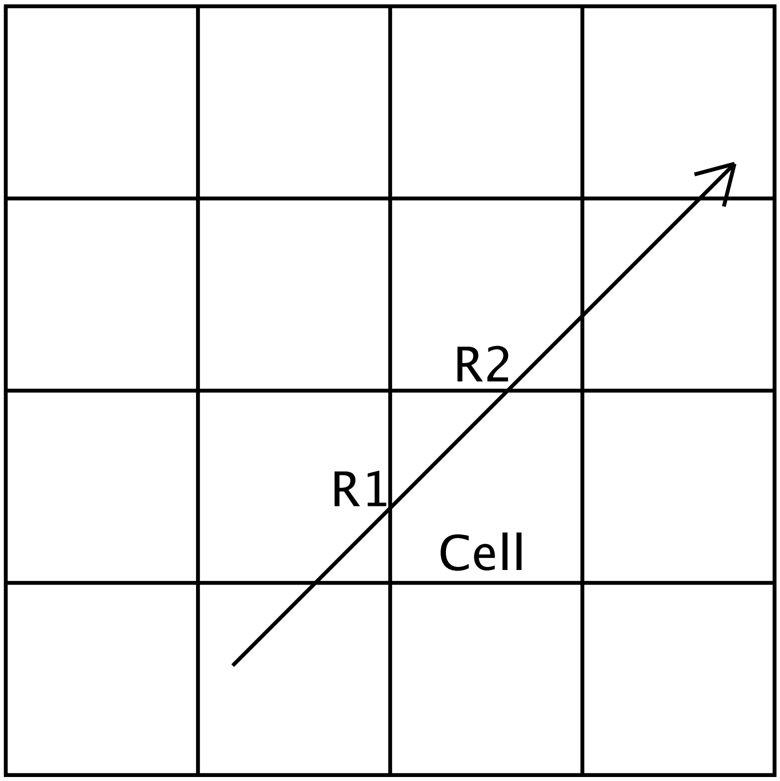

Figure 1. Idealized cell geometry for the n^{3}He ion chamber.

For ^{1}H, the energy as a function of residual range $E_1(R_1)$ can be determined by interpolation of a table of { R_1, E_1 } from the NIST pstar program. The dependence of range on energy, $R_1(E_1)$, can be constructed by interpolation of { E_1, R_1 }.

The ^{3}H range vs. energy is directly related to the ^{1}H range through the relationships

$$R_3(E_3) = \int_0^{E_3} \frac{dU}{dE/dX(E_3/3)} =$$

$$3\int_0^{E_3/3} \frac{dV}{dE/dX(V)} = 3R_1(E_3/3)$$

One can then construct a table of { E_3, R_3 } and determine the energy vs. range for ^{3}H in He, $E_3(R_3)$ by interpolation.

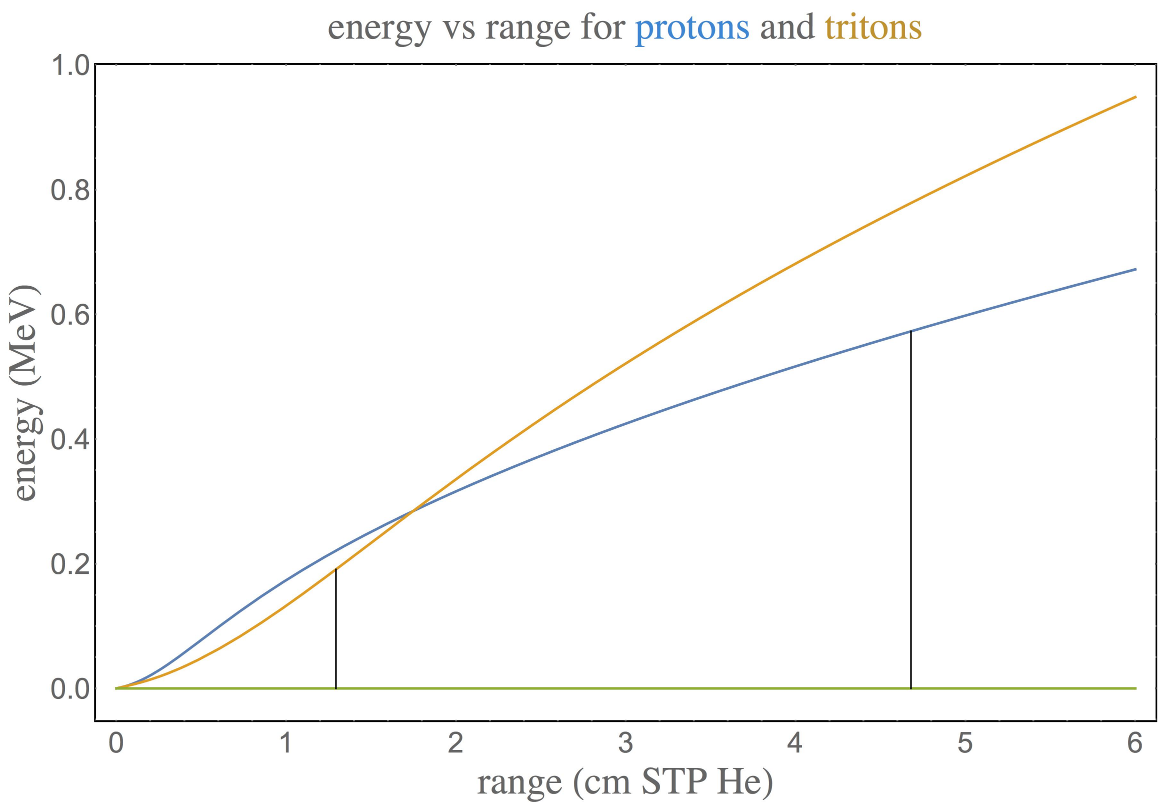

Figure 2. E vs. R for ^1H and ^3H in He. Note that the units of the x axis are independent of the isotope of He. The vertical lines are at the ranges of the reaction products of $n + {}^3He \rightarrow p + {}^3H$.

6B.

We measure the charge collected from the motion of electron ion pairs, not the energy loss. We must estimate this effect. For projectile velocities large compared to that of atomic electrons, the energy loss is due to ionization, while for projectile velocities small compared to that of atomic electrons, the energy loss is due to target recoil and transitions between atomic bound states. The same considerations lead to the maximum of the *dedx(E)* having a maximum at *E*=80 keV/AMU. We need to understand this issue better. A scoping calculation is to compare the quality of fits to the jaw-scan data to the dedx(E) and dedx(E) cut off below 80 keV.

I researched the dependence of W (the energy to create an electron-ion pair.

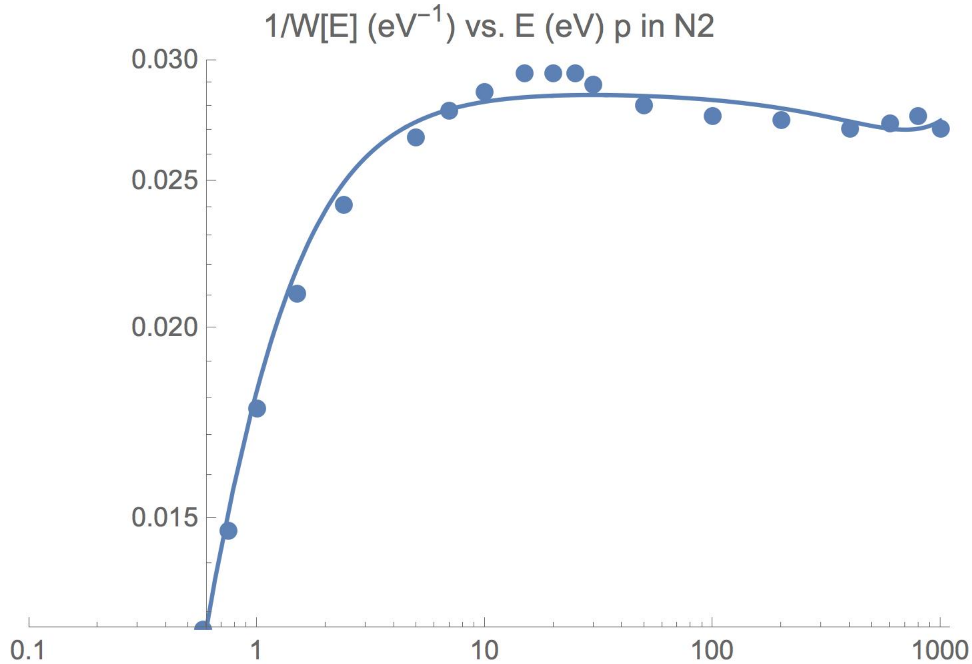

1/W[E] vs E for p in N2. The variation of W with E is small. I couldn't find data for p in He. I plotted p in N2. Data for other gasses including Ar are similar.

I expect the dependence of the geometric factors and jaw scans on the variation of W to be ~ 1 %. We can check this expectation by performing simulations using constant W and the N2 data.

6C.

There are 2 ranges defined in the NIST tables.

1. CSDA range. The fluctuations in the projectile direction straightened out.
2. Projected range. The range is the projection of the endpoint of the range on the initial direction. The "Detour Factor" is the ratio of Projected to CSDA.

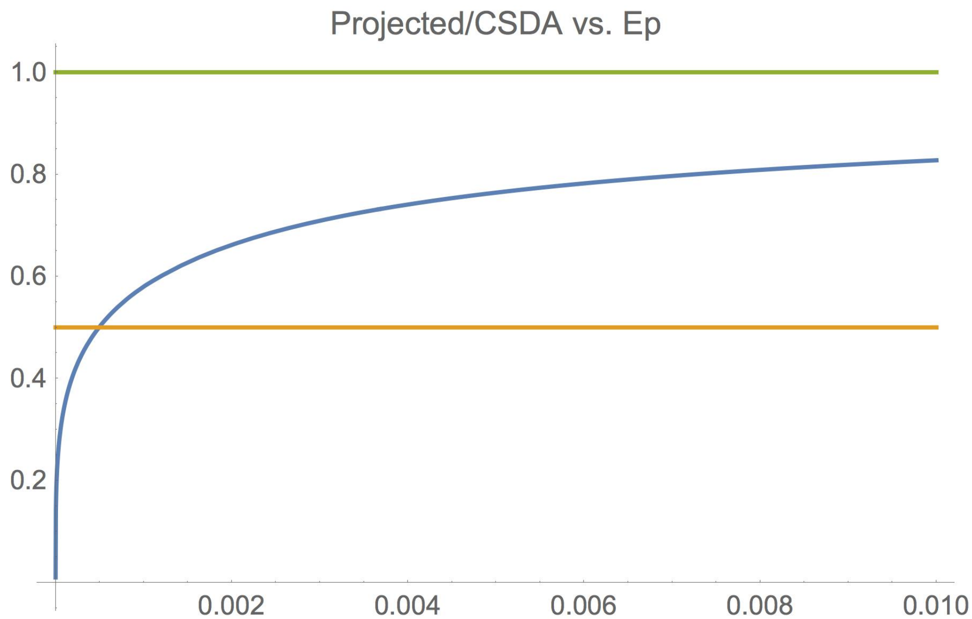

The Detour factor = .5 at an energy of .5 keV. I conjecture that this effect is negligible because for such small energies, the projectile is no longer producing ionization.

6D.
I looked into the Shockley-Ramo theory of charge collection (in Knoll). I concluded that although the time-profile of charge collection depends on the details of the electric field in an ion chamber, the total collected charge is determined by the charges that actually end up on the electrodes. This is what we have assumed. Mark reported some contrary findings, and I have written to him and asked for an update.

The only remaining open issues is:
Carry out simulations of geometric factors and jaw scan results using the above energy vs. range data from NIST PSTAR and different assumptions for W. One code would do both. Compare the jaw scan simulations with experimental results. If we find agreement, we can argue that we have tested the validity of the calculation of geometric factors.